Journal of Building Engineering 63 (2023) 105524

Contents lists available at ScienceDirect

Journal of Building Engineering

journal homepage: www.elsevier.com/locate/jobe

Multi-parametric flowability classification of self-compacting concrete containing sustainable raw materials: An approach to real applications

Víctor Revilla-Cuesta [a], Marta Skaf [b,*], Vanesa Ortega-López [a], Juan M. Manso [a]

[a] Department of Civil Engineering, Escuela Politécnica Superior, University of Burgos, c/ Villadiego s/n, 09001, Burgos, Spain
[b] Department of Construction, Escuela Politécnica Superior, University of Burgos, c/ Villadiego s/n, 09001, Burgos, Spain

ARTICLE INFO

Keywords:
Self-compacting concrete
Sustainable raw material
Multi-parametric flowability classification
Overall flowability
Flowability balance
Flowability predominance

ABSTRACT

Adding sustainable raw materials to Self-Compacting Concrete (SCC) modifies its flowability behavior. Furthermore, the use of these raw materials may at the same time even improve one fresh property while worsening another. An accurate flowability description of SCC containing sustainable raw materials therefore requires a multi-parametric classification that simultaneously covers all fresh properties (slump flow, viscosity, and blocking ratio) for an accurate description of its potential applications. Existing classifications consider each fresh property independently. In this paper, a multi-parametric flowability classification of SCC containing sustainable raw materials is proposed. The effects of multiple sustainable raw materials on SCC flowability are compiled in a dataset serving as a knowledge base with information on 663 SCC mixes containing sustainable aggregates and binders. The statistical analysis of the dataset led to the definition of three types of flowability zones. Firstly, the overall-flowability zones, in which SCC flowability is described in absolute terms: the better the in-fresh properties, the better the overall-flowability zone. Secondly, the flowability-balance zones reflect the balance between free flow (slump flow and slump-flow viscosity) and flow around obstacles (V-funnel emptying time and L-box blocking ratio). Finally, SCC is classified within flowability-predominance zones, which define the main characteristic of SCC flowability, rate of flow (viscosity) or uniformity of flow (spreading). The variability of the effect of each sustainable raw material on the flowability of SCC makes this classification useful, in so far as it offers a complete picture of the fresh behavior of SCC in which all fresh properties are simultaneously considered. Furthermore, based on the description in the proposed classification of overall flowability and the balance between free flow and flow around obstacles, the application fields are defined for which the use of each SCC mix with sustainable raw materials is recommended.

1. Introduction

Self-Compacting Concrete (SCC) has specific advantages over other types of concrete in relation to its placement. Its high in-fresh flowability is the distinctive feature of its behavior, which is appropriate for on-site placement without vibration [1]. Thus, concreting can be easily performed in almost any situation, even where elevated pumping heights are required and operator access is difficult [2].

* Corresponding author.
E-mail addresses: vrevilla@ubu.es (V. Revilla-Cuesta), mskaf@ubu.es (M. Skaf), vortega@ubu.es (V. Ortega-López), jmmanso@ubu.es (J.M. Manso).

https://doi.org/10.1016/j.jobe.2022.105524
Received 30 August 2022; Received in revised form 24 October 2022; Accepted 7 November 2022
Available online 10 November 2022
2352-7102/

The high flowability of SCC also means that its use has environmental advantages [3], because the absence of vibration when using SCC results in significant energy saving during placement [4], which in turn translates into a notable reduction of its carbon footprint [5]. Thus, SCC is a highly desirable type of concrete, because of its operational and functional advantages and its higher sustainability than other concrete types.

In the fresh state, concrete is classified according to its slump in the Abrams-cone test, EN 12350-2 [6], which is an indicator of its ease of placement. According to Standard EN 206 [6], there are five consistency classes: *S1* (slump between 10 and 40 mm); *S2* (slump between 50 and 90 mm); *S3* (slump between 100 and 150 mm); *S4* (slump between 160 and 210 mm); and *S5* (slump higher than 220 mm). On the basis of that classification, SCC is a concrete with an *S5 consistency class*. However, this classification is insufficient for SCC, since the absence of vibration during concreting implies that this type of concrete must settle on its own as effectively as vibrated concrete [7]. Thus, SCC must, without applying any vibration or external force, be able to flow/spread (free-flow capability) at an adequate rate of flow (viscosity), to flow around obstacles, such as reinforcement bars (passing ability), and must present no segregation between its different components [8]. A situation that has resulted in the development of different fresh-state tests, each of which measures one of the above-mentioned aspects [1]. It has likewise led to the existence of several classifications for SCC, one for each of the above aspects, as shown in Table 1.

In SCC containing conventional raw materials (natural aggregate and ordinary Portland cement), it is common to use single-parameter flowability classifications, in which the different fresh properties are not interrelated with each other [9]. Each SCC mix is therefore assigned six classifications, one for each fresh property that is measured [1], as shown in Table 1. This procedure is valid because, in general, there is a directly proportional relation between all characteristics, *i.e.*, the improvement of one of these properties, *e.g.*, slump flow (free-flow capability), implies the improvement of the others (viscosity and passing ability) [10]. Although multi-parametric flowability classifications have been shown to provide a more complete and a simpler overview of SCC flowability, efforts to develop them are very scarce, the most relevant example being *"Okamura's map"* [11]. On this map, the SCC is represented within a two-dimensional space, whose dimensions are the relative slump flow and the relative slump-flow viscosity of the mortar phase of the SCC mix [11]. Through those two parameters, the mixtures can be classified as having *"excellent behavior"* (AA), *"good*

Table 1
Standard classification of SCC.

Test	Standard [6]	Measured parameter	SCC property evaluated	Classification [1,6]
Slump-flow test	EN 12350-8	Final spreading diameter (slump flow)	Free-flow capability	Slump-flow class • SF1: final spreading diameter between 550 and 650 mm • SF2: final spreading diameter between 650 and 750 mm • SF3: final spreading diameter between 750 and 850 mm
Slump-flow test	EN 12350-8	Time to reach a spreading diameter of 500 mm (t_{500})	Free-flow viscosity	Slump-flow viscosity class • VS1: 500-mm-slump-flow time lower than 2 s • VS2: 500-mm-slump-flow time higher than 2 s
V-funnel test	EN 12350-9	V-funnel emptying time	Rate of flow (viscosity) when overcoming obstacles	V-funnel viscosity class • VF1: V-funnel emptying time between 0 and 8 s • VF2: V-funnel emptying time between 9 and 25 s
L-box test	EN 12350-10	Blocking ratio (ratio between the heights at the beginning and at the end of the box)	Passing ability	Passing-ability class • PA1: blocking ratio higher than 0.80 in a 2-bar L-box • PA2: blocking ratio higher than 0.80 in a 3-bar L-box
Sieve-segregation test	EN 12350-11	Percentage loss of mass through a 5-mm-opening sieve	Segregation resistance	Segregation-resistance class • SR1: percentage mass loss lower than 20% • SR2: percentage mass loss lower than 15%
J-ring test	EN 12350-12	(1) Final diameter spreading (2) Height difference inside and outside the J-ring	(1) Free-flow capability (2) Passing ability	J-ring slump-flow class, as in the slump-flow test J-ring slump-flow viscosity class, as in the slump-flow test J-ring passing-ability class • PJ1: height difference lower than 10 mm in a 12-bar J-ring • PJ2: height difference lower than 10 mm in a 16-bar J-ring

behavior" (A) and *"acceptable behavior"* (B) [12], as shown in Fig. 1.

Nowadays, the use of waste and by-products for the manufacture of any type of concrete, such as SCC, is a very common practice [8,13,14]. The replacement of conventional aggregates and cement with those materials is a highly recommendable practice from a sustainability point of view [14]. On the one hand, it reduces the numerous environmental impacts resulting from the manufacture of the conventional raw materials used in concrete, such as CO_2 emissions during Portland cement production [13] and land damage due to aggregate extraction from quarries and gravel pits [7]. On the other, it solves the problem of storage and consequent disposal in landfill sites of these wastes or industrial by-products [15]. However, if this practice is to be truly possible, there has to be a guarantee that whenever SCC contains waste and by-products its behavior will be adequate in both the fresh and the hardened state [14,16]. Numerous studies in the literature have reported successful results for SCC containing sustainable aggregates, such as copper-slag coarse and fine aggregate [17,18], steel-slag coarse and fine aggregate [19,20], recycled-concrete coarse and fine aggregate [8], and plastic-waste fine aggregate [21], and sustainable binders, such as fly ash [22], silica fume [23], and ground granulated blast furnace slag [23]. Thus, these wastes and by-products are considered as sustainable raw materials, in so far as SCC containing such materials behave in similar ways to SCC containing conventional raw materials and concrete sustainability is greater.

Although successful results have been obtained in relation to the behavior of SCC containing sustainable raw materials, their addition has modified the behavior patterns of SCC [24]. Focusing exclusively on the fresh behavior, unlike the SCC made with conventional raw materials, no directly proportional behavior has been found between the fresh properties listed in Table 1 when using sustainable raw materials [7,8,14]. A phenomenon that is a result of modifications to the SCC mix composition when adding sustainable raw materials and the different properties that each sustainable raw material presents:

- Increasing the content of coarse recycled concrete aggregate can in some cases worsen the slump-flow viscosity of SCC while improving the V-funnel viscosity. A behavior that was especially observed when the sustainable aggregate was pre-soaked before use [25].
- Additions of fine recycled concrete aggregate instead of natural siliceous sand can improve the slump flow of SCC, provided adequate particle sizes are used. However, the flow of the SCC slows down, *i.e.*, its viscosity increases [26].
- With only a small increase in its content, the high density of slag aggregate leads to improvements of both the slump flow and the ability of the SCC to flow around obstacles, although, at the same time, it increases viscosity [18]. The high density of slag aggregate, especially if this aggregate is used in very high quantities, can also lead to an increased risk of segregation between the aggregate and the cement paste, [27]. Adjusting the fine aggregate content and carefully controlling the segregation resistance of SCC are key aspects for solving these slag-aggregate-related issues [28].
- Other sustainable aggregates show no clear trends with regard to their effects on SCC flowability. For example, plastic aggregate in some cases improves both the slump flow and the viscosity of SCC [29], while in other cases it enhances the viscosity of SCC, but reduces its slump flow [30]. Results that can be explained by the lower density of plastic compared to natural aggregate, as well as its large variety of shapes. The same assertions can be made for glass aggregate [31].
- In some cases, when fly ash is used, the increase in the passing ability of SCC is accompanied by an increase in viscosity, while slump flow remains constant [32]. This behavior depends on the type of fly ash in use, the coarse-to-fine-aggregate ratio, and the proportion of added plasticizer [32,33].
- Finally, the lower grinding fineness of ground granulated blast furnace slag compared to conventional cement causes the slump flow to increase while the passing ability decreases [34]. Nevertheless, the specific behavior will depend on the mix design [26]. The same applies when silica fume is used [35].

Single-parameter flowability classifications, in which each fresh property of SCC is separately considered, cannot answer the following question, "*What is more important for the flowability behavior of SCC, an improvement in one fresh property or the worsening of another one?",* when adding any sustainable raw material [1]. Thus, the variability of the behavior of SCC containing those materials means that single-parameter classifications never quite accurately describe its flowability. It in turn means that their range of possible applications are not well defined. Multi-parametric flowability classifications therefore need to be developed, in which all the fresh characteristics of SCC containing sustainable raw materials are simultaneously considered and interrelated with each other. In this

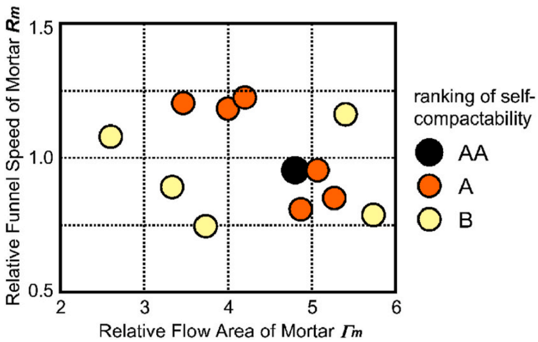

Fig. 1. Okamura's map [11].

way, it is possible to obtain a more complete picture of the fresh behavior of SCC. So far, this type of classification has not been studied in the literature, and only a few studies addressing workability boxes for certain types of waste are available [36].

2. Initial approach

As stated in the introduction, the aim of this paper is to provide a multi-parametric flowability classification of SCC that contains sustainable raw materials. A classification that is based on simultaneously considering all the fresh properties of this alternative SCC and their interrelations, rather than each property in isolation, as is usually the case for conventional SCC (Table 1). In this way, a classification will be presented that provides a full overview of the flowability of SCC containing sustainable raw materials.

The in-fresh properties of SCC that were considered for the development of the classification were slump flow, slump-flow viscosity, V-funnel emptying time, and L-box blocking ratio (passing ability). These properties provide insight into the behavior of the SCC in relation to its free flow (slump flow and slump-flow viscosity) and its movement when facing obstacles (holes, V-funnel emptying time, and reinforcements, L-box) [1]. The J-ring test was not considered, because it measures both the free-flow capability and the passing ability of SCC, and its use would unnecessarily complicate the interpretation of the classification, due to the interaction between those two fresh properties during that test [37]. Neither was segregation resistance considered, because it is not a measure of the capability of SCC to flow, but a measure of the cohesion between the components of SCC when fresh. It was therefore thought easier to maintain the classification used for conventional SCC (*classes SR1* and *SR2*, Table 1).

Having defined these aspects, a literature review was conducted of papers reporting the measurement of these four fresh properties (slump flow, slump-flow viscosity, V-funnel emptying time, and L-box blocking ratio) in an SCC containing sustainable raw materials, whether aggregate, aggregate powder (fraction 0/0.5 mm of the aggregate), or binder. These three types of sustainable raw materials were jointly considered for the development of the proposed multi-parametric classification, in order, on the one hand, to achieve the most generic possible classification and, on the other, to consider the flowability interactions that could exist between them when used simultaneously in the same SCC mix. In Table 2, the scientific papers containing the data with which the proposed classification was developed are shown alongside each sustainable raw material. Thus, a dataset of 663 SCC mixes containing sustainable raw materials was obtained. All the scientific papers under consideration had been published over the past few years, so the classification could be adapted to current practice when preparing SCC. From the results on the four fresh properties reported for each of these 663 SCC mixes, a statistical procedure based on extracting the principal dataset components was performed. This procedure, described in detail in the following section, yielded the multi-parametric flowability classification that is proposed in this study.

3. Multi-parametric flowability classification

In this section, the multi-parametric classification is developed by calculating the principal components of the fresh properties of the dataset of 663 SCC mixes. A brief explanation of the method precedes the presentation of the results from which the classification was developed.

3.1. Principal-components procedure

Let us suppose that there is a set of m elements (in this case, 663 SCC mixtures) for which n properties or characteristics have been measured (in this case, 4 fresh properties: slump flow, slump-flow viscosity, V-funnel emptying time, and L-box blocking ratio). Furthermore, no precise relationship between any of the n properties can be established when considering the values of the n properties of the m elements. This situation hinders the m elements from being successfully grouped/classified within a space of less than n dimensions. One dimension would have to be considered for each property to be measured, in order to group/classify the m elements, all of which makes the classification very difficult to interpret.

Table 2
Knowledge base for the study.

Component	Sustainable raw material	Mixes of the knowledge base with the sustainable raw material (%)[a]	References
Aggregate	Slag aggregate	33.2	[17,18,28,34,38–49]
	Recycled concrete aggregate	37.5	[2,5,25,26,33,37,42,50–66]
	Plastic aggregate	8.9	[29,30,67–71]
	Glass aggregate	4.1	[31,72–74]
	Rubber aggregate	3.4	[70,72,75,76]
	Ceramic aggregate	2.9	[67,70,77]
Aggregate powder	Slag powder	2.4	[47,66,78]
	Recycled concrete powder	7.6	[26,50,51,79]
	Glass powder	2.2	[28,49,80,81]
	Ceramic powder	3.4	[67,78,82,83]
Binder	Fly ash	45.9	[17,30,32,33,35,38,39,41,43,44,46–48,50–54,57–62, 64,70,73,77,79,84–89]
	Ground granulated blast furnace slag	36.8	[26,32,34,40,42,45,46,49,61,82–87,89–91]
	Metakaolin	8.1	[31,41,50,52,53,61,91]
	Silica fume	18.7	[17,30,35,40,41,49,51–53,59,64,76,79,83,87]

[a] The sum of the percentages is not 100% due to the existence of mixes that simultaneously contain two or more sustainable raw materials.

Principal-components analysis is a statistical method that consists of constructing fictitious quantities, called principal components, that are linear combinations of *n* properties measured for *m* elements. Each principal component describes a certain percentage of the variance of the dataset. This variability defines the coefficients of each property for each principal component [92].

As many principal components as there are measured properties would explain 100% of the variance of the data, *i.e.*, *n*. However, with a smaller number of principal components, it is possible to cover 70–80% of the variability of the data that is normally considered sufficient [92,93]. Thus, it is possible to explain the behavior of *m* elements with a smaller number of variables, grouping them in a space of as many dimensions as there are principal components needed to explain 70–80% of the variance [93]. In our case, SCC mixes need 4 fresh properties for an adequate description of their behavior (four-dimensional space), although their flowability behavior can be successfully described with only 2 principal components (two-dimensional space) as shown in the following sections.

The principal components need no interpretation; they are simply linear combinations of *n* measured properties. However, a useful classification will be one in which the principal components have an easy and direct interpretation, as with those presented in this study.

Finally, it is important to note that the principal components are calculated with the normalized values of the properties considered in the analysis (values between 0 and 1). Therefore, when defining a principal component, each value of each property is subtracted from the mean and divided by the standard deviation calculated from the values of that property for all the *m* elements. Therefore, the formula of the principal components is conditioned by the specific *m* elements used to obtain them [92]. However, if properties needing no normalization (*i.e.*, their values are already between 0 and 1) are used, then instead of directly using the value of the properties and subsequently normalizing them to obtain the principal components, the application of the principal components is much more generic and valid for elements not introduced in the principal-components analysis.

3.2. Normalized fresh properties

Rather than considering the traditional slump-flow, viscosity and passing-ability classes (Table 1), it was necessary to work with the values of the different fresh properties, in order to prepare a classification in which all the fresh properties would be simultaneously considered so that it would be widely applicable. Bearing in mind the usefulness of normalizing the fresh properties before obtaining the principal components, an aspect explained in the previous section, the 4 fresh properties under consideration were therefore normalized, *i.e.*, transformed to assume values between 0 and 1 in a linear way with the experimental values of the fresh properties. In addition, the normalized properties were set to a value of 0 for the worst value of the fresh property and 1 for the most favorable value, so that they could be intuitively understood. Finally, two other aspects were also considered to preserve the range of SCC fresh property values included in the standards [1]:

- If a property had a worse value than the most unfavorable value in the standards, EN 206 [6], *i.e.*, a slump flow lower than 550 mm, a blocking ratio lower than 0.80, or a V-funnel emptying time higher than 25 s, then the normalized property took the value of 0. A maximum value of t_{500} is not considered in the definition of the slump-flow-viscosity classes of the regulations, which is necessary to normalize the value of t_{500}. Therefore, 5 s was established as the most unfavorable value based on the authors' experience and on the behavior of the SCC observed in the literature [7,8,21–23].
- If a fresh property had a better value than the most favorable value in the standards, EN 206 [6], *i.e.*, a slump flow higher than 850 mm, then the normalized fresh property assumed a value of 1.

Each normalized fresh property, designated with a subscript '*s*', was calculated with a different equation: Equation (1) for slump flow (*SF*, in mm); Equation (2) for slump-flow viscosity (*SFV*, in seconds); Equation (3) for V-funnel emptying time (*VFV*, in seconds); and Equation (4) for L-box blocking ratio (*BR*, dimensionless).

$$\begin{cases} 0 \quad SF < 550 \\ SF_s = \dfrac{SF - 550}{300} \quad 550 \le SF \le 850 \\ 1 \quad SF > 850 \end{cases} \tag{1}$$

$$\begin{cases} SFV_s = \dfrac{5 - SFV}{5} \quad 0 \le SFV \le 5 \\ 0 \quad SFV > 5 \end{cases} \tag{2}$$

$$\begin{cases} VFV_s = \dfrac{25 - VFV}{25} \quad 0 \le VFV \le 25 \\ 0 \quad VFV > 25 \end{cases} \tag{3}$$

$$\begin{cases} BR_s = \dfrac{BR - 0.80}{0.20} \quad 0.80 \le BR \le 1.00 \\ 0 \quad BR < 0.80 \end{cases} \tag{4}$$

3.3. Principal components

The principal-components analysis was performed using the previously normalized fresh properties of the 663 SCC mixes (see previous section) that formed the knowledge base. No further normalization of the fresh property values had to be performed. The ranges of values of the principal components were defined by maximizing the percentage of variance explained by the first two principal components, so that the classification would be as accurate as possible, while at the same time easy to apply. Thus, the two most relevant principal components (two first principal components) were set at positive values of between 0 and + 2 so that they only had values in the first quadrant of the two-dimensional plane, which simplified the classification. In addition, the values of the third principal component had to be within a range of 2 units with values between −1 and +1 to uniformize the width of the range of values of all the principal components, so as to avoid mistakes.

Bearing in mind the aspects described in the previous paragraph and applying the statistical procedure for obtaining the principal components of a dataset, the principal components of the SCC-mix knowledge base were generated using statistical software. These are shown in Equation (5) (first principal component, PC_1), Equation (6) (second principal component, PC_2), and Equation (7) (third principal component, PC_3). The fourth and last principal component was considered of no use, as the flowability classification was not simplified when using as many principal components as fresh properties, so it was therefore omitted.

$$PC_1 = 0.09 \times SF_s + 0.11 \times SFV_s + 0.74 \times VFV_s + 1.06 \times BR_s \tag{5}$$

$$PC_2 = 0.80 \times SF_s + 1.00 \times SFV_s + 0.04 \times VFV_s + 0.16 \times BR_s \tag{6}$$

$$PC_3 = -0.48 \times SF_s + 0.13 \times SFV_s + 0.87 \times VFV_s - 0.52 \times BR_s \tag{7}$$

The principal components presented a simple interpretation related to the fresh behavior of SCC containing sustainable raw materials:

- The first principal component reflected the ability of the SCC containing sustainable raw materials to flow around obstacles, both through holes (V-funnel test) and around reinforcements (L-box test). It can be observed from the results of Equation (5) that the higher the normalized fresh properties VFV_s and BR_s, *i.e.*, the lower the V-funnel emptying time and the higher the L-box blocking ratio, then the higher the principal-component value.
- Similarly, the second principal component reflected the free-flow capability of SCC containing sustainable raw materials, so that the higher its value, the higher the free-flow capability of the SCC. Equation (6) shows that this principal component was mainly dependent on the normalized fresh properties SF_s and SFV_s.
- Finally, the third principal component served to compare the uniformity of flow (slump flow and L-box blocking ratio) of the SCC containing sustainable raw materials with its rate of flow or viscosity (slump-flow viscosity, t_{500}, and V-funnel emptying time). Thus, if the third principal component has positive values (between 0 and + 1), it is the rate of flow of the SCC mix that predominates, rather than its uniformity of flow. However, if this principal component has negative values (between −1 and 0), then the situation is reversed, and it is the uniformity of flow that predominates over the rate of flow.

The results of the first two principal components were sufficient to explain 75.0% of the variance of the data, an adequate value in common practice [93]. Therefore, a two-parameter flowability classification, *i.e.*, a two-dimensional classification, can be constructed from them. If the third principal component is also used, 92.5% of the variance of the data can be explained and its use enables the above two-dimensional classification to be completed, resulting in a three-parameter flowability classification (three-dimensional classification).

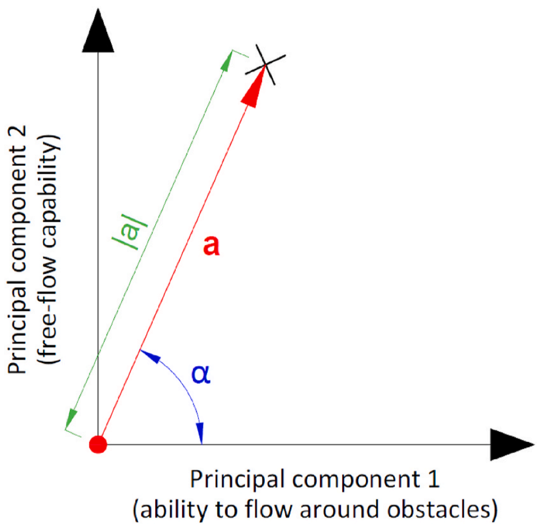

Fig. 2. Polar coordinates.

3.4. Two-parameter flowability classification (two-dimensional classification)

The variance percentage explained by the first two principal components (PC_1 and PC_2) is suitable for a two-dimensional Cartesian representation of the SCC mixes. In this representation (Fig. 2), each principal component defines the value on each axis. The first principal component (Equation (5)) is represented on the x-axis, while the second principal component defines the value on the y-axis (Equation (6)). Furthermore, according to the definition of the principal components, every pair of points was in the first quadrant of the two-dimensional Cartesian system. The maximum value on each axis was 2.

However, a simple grouping of the mixes could not be represented with these Cartesian coordinates. For this reason, it was decided to use polar coordinates (Fig. 2). The SCC mixes containing sustainable raw materials were therefore classified in terms of both the modulus of the vector from the origin to the analyzed point and the angle that the vector forms with the x-axis. These two parameters, $|a|$ (modulus) and α (angle), are represented in Fig. 2 and formulated in Equation (8) and Equation (9), respectively.

$$|a| = \sqrt{(PC_1)^2 + (PC_2)^2} \tag{8}$$

$$\alpha = \tan^{-1}\left(\frac{PC_2}{PC_1}\right) \tag{9}$$

The two-parameter flowability classification was therefore defined in terms of the values of the polar coordinate parameters, $|a|$ and α.

3.4.1. Overall-flowability zones

The modulus of the vector, parameter $|a|$, is a measure of SCC flowability from a global point of view. It can be considered as an average value of the four normalized fresh properties. Although the parameter entails no evaluation of the balance between the ability to flow around obstacles (first principal component) and the free-flow capability (second principal component), it provides an initial overall flowability estimation of SCC containing sustainable raw materials. As the values of both the first and the second principal component were set to vary between 0 and 2, the value of the parameter $|a|$ ranges between 0 and 2.83. Considering this range of values and dividing it into equal probability percentiles, according to the $|a|$ parameter values of all 663 mixes that constituted the knowledge base for this study, yielded five overall-flowability zones, which are defined and detailed in both Table 3 and Fig. 3.

These overall-flowability zones enable an initial classification of the SCC mixes containing sustainable raw materials according to the SCC mix fresh behavior. They were obtained through a review of the conclusions on in-fresh behavior found in the articles that composed the knowledge base (Table 2):

- *Zone 1* ($|a|>2.47$) can be qualified as *"ideal"* due to the high values needed for all four normalized fresh properties simultaneously. It represents the optimal type of SCC containing sustainable raw materials for any application. Although this overall-flowability zone can be calculated in both mathematical and statistical terms, the development of an SCC containing sustainable raw materials that has this "*ideal*" behavior is almost impossible in practice. In fact, none of the 663 mixes listed in the dataset (Table 2) had an $|a|$ parameter value that met the required value for classification within this zone.
- *Zone 2* ($2.10<|a|<2.47$) corresponds to the *"real optimal"* SCC containing sustainable raw materials, *i.e.*, SCC which presents optimal flowability for use and can actually be developed in practice [11]. The SCC with this overall-flowability class could be used for any type of building application, although its main area of application should be for pumping concrete to form beams and columns at great heights.
- Mixes in *Zone 3* ($1.40<|a|<2.10$) showed *"good"* overall flowability, the one that has most commonly provided good results in practice in view of current experience [1]. It is therefore the recommended overall-flowability class in absolute terms, without separate consideration of free-flow capability and ability to flow around obstacles. According to the literature [56], an SCC with this overall-flowability class could be used in the precast-concrete industry to manufacture building elements, although its *in-situ* use is also suitable, but using it for lower pumping heights than a *Zone 2* SCC.
- When in *Zone 4* ($0.70<|a|<1.40$), it refers to an SCC of *"acceptable"* overall flowability. It can be used but only with caution, attentive to its real behavior during placement and whether vibration is required.
- Finally, an SCC containing sustainable raw materials in *Zone 5* ($|a|<0.70$) will have very low flowability and, in extreme cases, an absence of self-compactability. Its use is not therefore recommendable.

Table 3
Overall-flowability zones.

Code	Parameter intervals	Description [a]
1	**$\|a\|>2.47$**	All normalized values of SCC fresh properties above 0.87
2	**$2.10<\|a\|<2.47$**	All normalized values of SCC fresh properties between 0.75 and 0.87
3	**$1.40<\|a\|<2.10$**	All normalized values of SCC fresh properties between 0.50 and 0.75
4	**$0.70<\|a\|<1.40$**	All normalized values of SCC fresh properties between 0.25 and 0.50
5	**$\|a\|<0.70$**	All normalized values of SCC fresh properties values below 0.25

[a] Not all fresh properties will have these values as these are average values. Thus, if a normalized fresh property has a lower value than required in one zone, a higher value of another normalized fresh property can compensate for it.

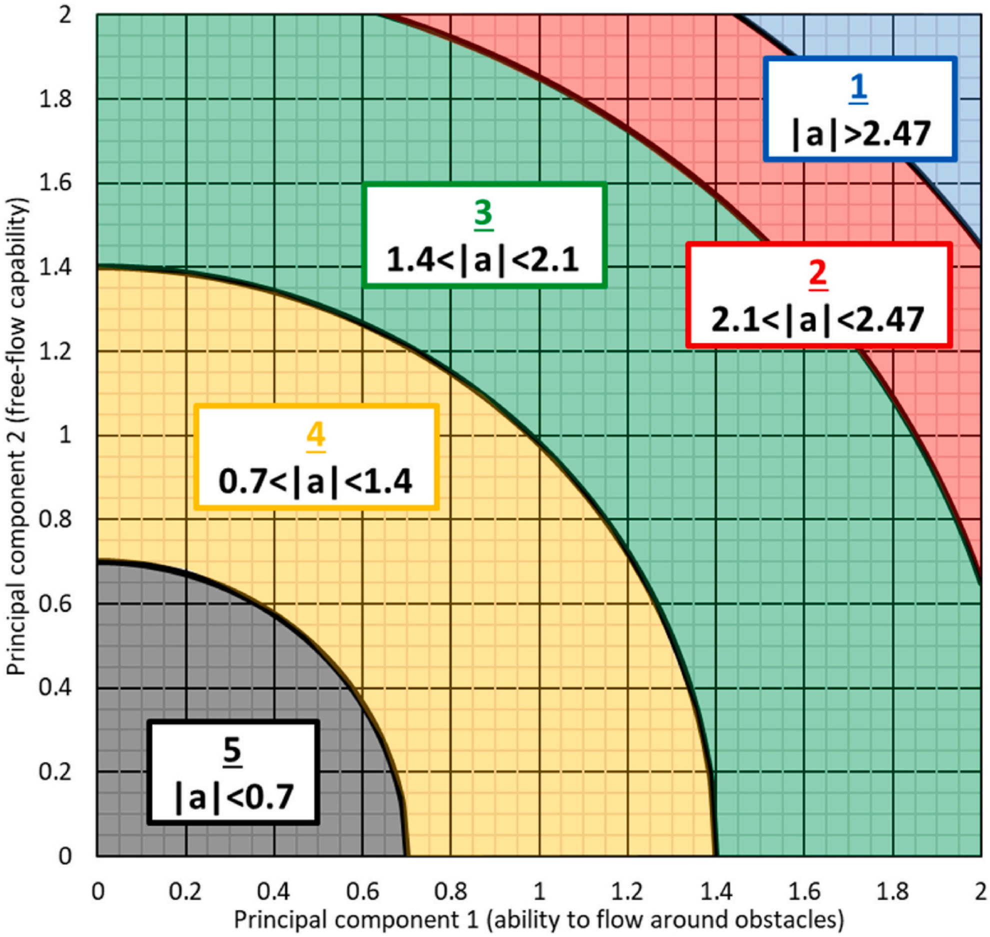

Fig. 3. Overall-flowability zones.

3.4.2. *Flowability-balance zones*

As the first two principal components will always be positive values, any combination of their values will be in the first quadrant of the two-dimensional Cartesian representation. Thus, the vector angle, parameter α, will always present values between 0° and 90°. The five flowability-balance zones were defined on the basis of the range of the α angle values, which were divided into five equal probability percentiles according to the values of the normalized fresh properties of all 663 SCC mixes in the knowledge base (Table 2). The coding of these zones, their corresponding α values, and their descriptions are shown in Table 4. These zones, graphically represented in Fig. 4, present comparisons of the passing ability (flow around obstacles) with the free-flow capability of an SCC mix containing sustainable raw materials.

The recommended fields of application for SCC with sustainable raw materials could be established for each flowability-balances zone, on the basis of these flowability-balance zones and the conclusions on the in-fresh behavior reported in the articles forming the knowledge base of the dataset (Table 2):

- An SCC containing sustainable raw materials that is in *Zone A* ($36° < \alpha < 54°$) is an SCC that can be successfully used for any application, guaranteeing a formwork-filling capability (free-flow capability) balanced with the ability to pass between

Table 4
Flowability-balance zones.

Code	Parameter intervals	Description
A	**36°<α<54°**	Adequate balance between free-flow capability and ability to flow around obstacles
B	**54°<α<72°**	Slightly better free-flow capability than ability to flow around obstacles
C	**18°<α<36°**	Slightly better ability to flow around obstacles than free-flow capability
D	**72°<α<90°**	Almost null ability to flow around obstacles compared to free-flow ability
E	**0°<α<18°**	Almost null free-flow capability compared to its ability to flow around obstacles

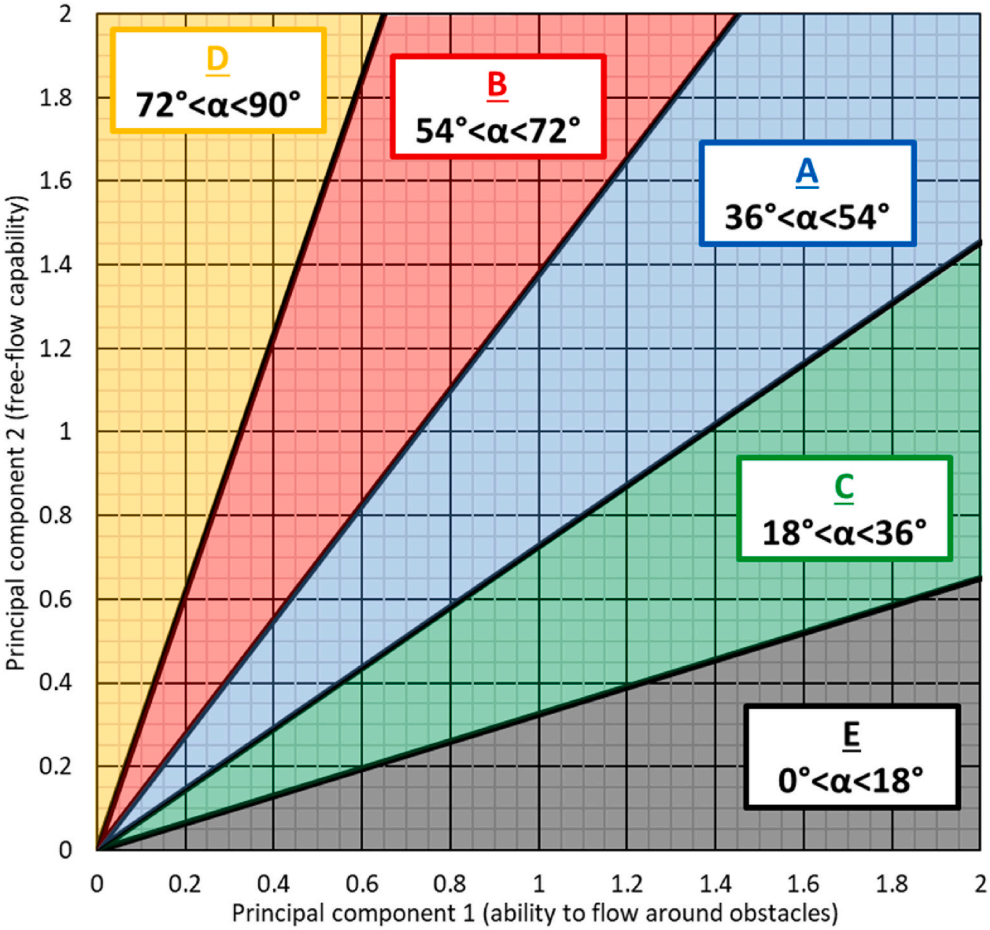

Fig. 4. Flowability-balance zones.

reinforcements (related to the L-box test) and its ability to be pumped (indirectly measured by the V-funnel test). It is the ideal flowability-balance zone, so this type of SCC could be used in any building application.

- Although they can be used in any application, the SCC mixes within *Zone B* and *Zone C* highlight the recommended fields of application. Mixes within *Zone B* ($54^\circ < \alpha < 72^\circ$) show a predominance of free-flow capability, and formwork-filling. Thus, in those situations where gutter pouring is required and when concreting large components with conventional reinforcement, such as footings and foundation slabs, it is advisable to use mixes within *Zone B.* In contrast, the first principal component of the mixes within *Zone C* ($18^\circ < \alpha < 36^\circ$) reflects the predominance of the ability to flow around obstacles. It is therefore advisable to use *Zone-C* mixes when placing by pumping or when concreting highly reinforced elements. Thus, *Zone-C* mixes are recommended for pumped concreting of tall buildings and singular elements with a complex shape, such as some roof types.
- In the SCC mixes of *Zone D* ($72^\circ < \alpha < 90^\circ$) and *Zone E* ($0^\circ < \alpha < 18^\circ$), the free-flow capability predominates very markedly over the passing ability or the ability to flow around obstacles or *vice-versa.* Therefore, these SCC mixes show unbalanced behavior that may involve disadvantages, such as the need for vibration. The use of such mixes is therefore not recommendable.

3.4.3. *Complete classification*

Both the overall-flowability zones and the flowability-balance zones provide very relevant information regarding the practical application of SCC containing sustainable raw materials. However, a complete picture of mix flowability is never provided from their isolated use alone:

- The overall-flowability zones refer to global flowability, without differentiating between the free-flow capability and the ability to flow around obstacles. Thus, the overall flowability of a mix may be very good in terms of a high slump flow, even though its V-funnel emptying time may be prolonged.
- The flowability-balance zones provide insight into whether the flowability of the SCC is balanced in terms of free-flow capability and ability to flow around obstacles. However, there is no indication of whether the overall flowability of the SCC containing sustainable raw materials is high.

A classification based on both parameters, $|a|$ and α, must therefore be applied, i.e., assigning an overall-flowability class and a flowability-balance class to each SCC mixture. Fig. 5 shows these combined zones together with their coding, combining what is separately established for each zone. Thus, for example, a Class-2A SCC mix is a mix with optimum flowability and balance between free flow and flow around obstacles (the ideal mix type from a practical point of view); a Class-3C mix is of “good” overall flowability, recommended for pumping and concreting of highly reinforced elements; and a mix of Class 4B is a mix with “acceptable” overall flowability that should be carefully monitored during placement and which is recommended for use in gutter pouring and when concreting highly reinforced elements.

Finally, it is worth noting the zones to which it is recommended that the SCC with sustainable raw materials belongs for an optimal on-site placement, which are marked with a red line in Fig. 5. On the one hand, an SCC in overall-flowability Zone 1 is almost impossible to obtain in practice, while an SCC in Zone 5 is very unlikely to be successfully placed. On the other hand, SCC mixtures that are in *flowability-balance zones D* and *E* show unbalanced behavior, with free-flow capability far exceeding the ability to flow around obstacles or *vice-versa*. Therefore, an SCC containing sustainable raw materials must be in zones *2A*, *2B*, *2C*, *3A*, *3B*, *3C*, *4A*, *4B,* and *4C* for successful placement.

3.5. Three-parameter flowability classification (three-dimensional classification)

The two-parameter flowability classification outlined above can be completed by considering the third principal component (PC_3, Equation (7)). It is used to establish a three-parameter classification through cylindrical coordinates in a three-dimensional space in which each dimension is a principal component (Fig. 6).

This three-parameter flowability classification consists of completing the overall-flowability and flowability-balance zones previously obtained (two-parameter classification) with flowability-predominance zones (Fig. 7). These zones depend on whether the third principal component (PC_3, Equation (7)) is either positive or negative:

- If the third principal component is positive, then the normalized values of the fresh properties related to rate of flow (slump-flow viscosity and V-funnel emptying time) will be higher than those more related to the uniformity of flow (slump flow and L-box blocking ratio). Rate of flow therefore predominates in an SCC containing sustainable raw materials with a third principal component greater than 0. These SCC mixes can be coded with an *"s"* (speed, rate of flow-predominance zone).

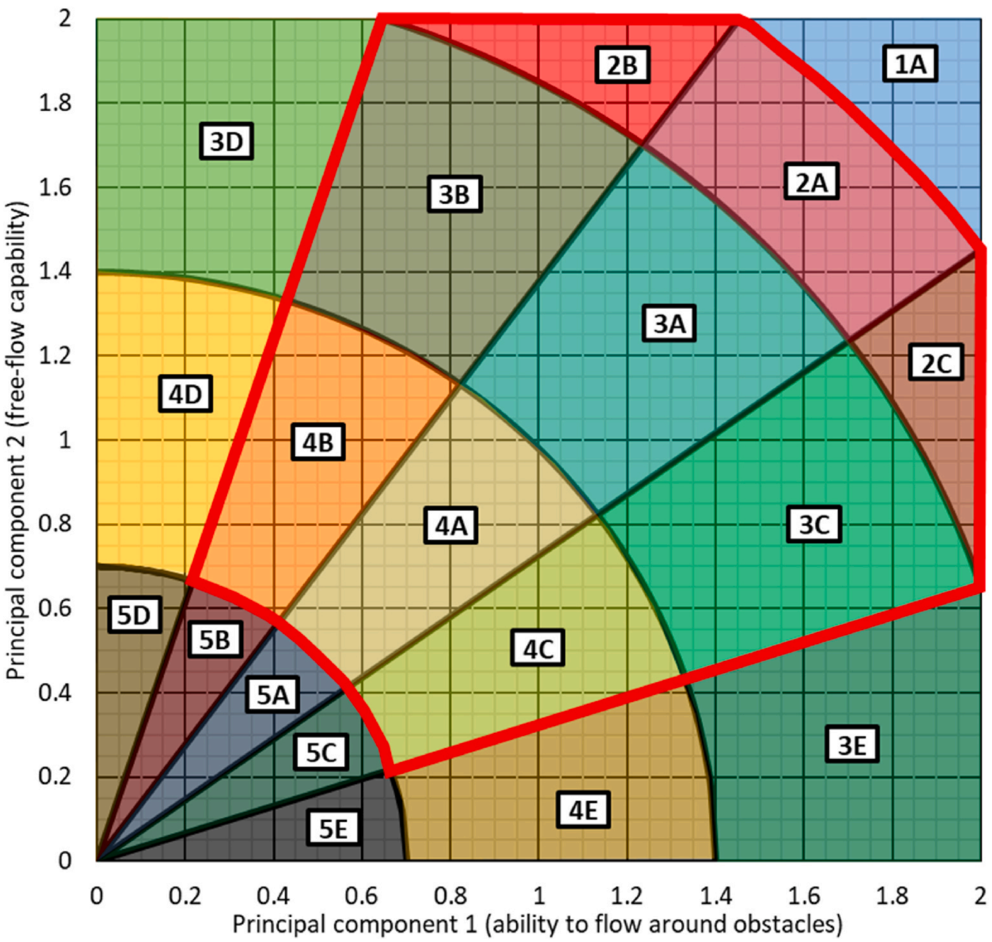

Fig. 5. Complete classification.

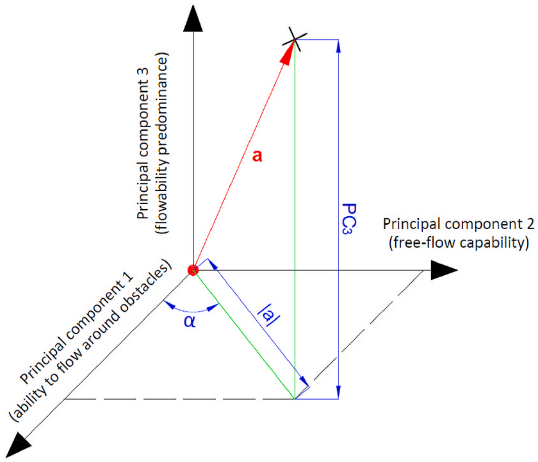

Fig. 6. Cylindrical coordinates.

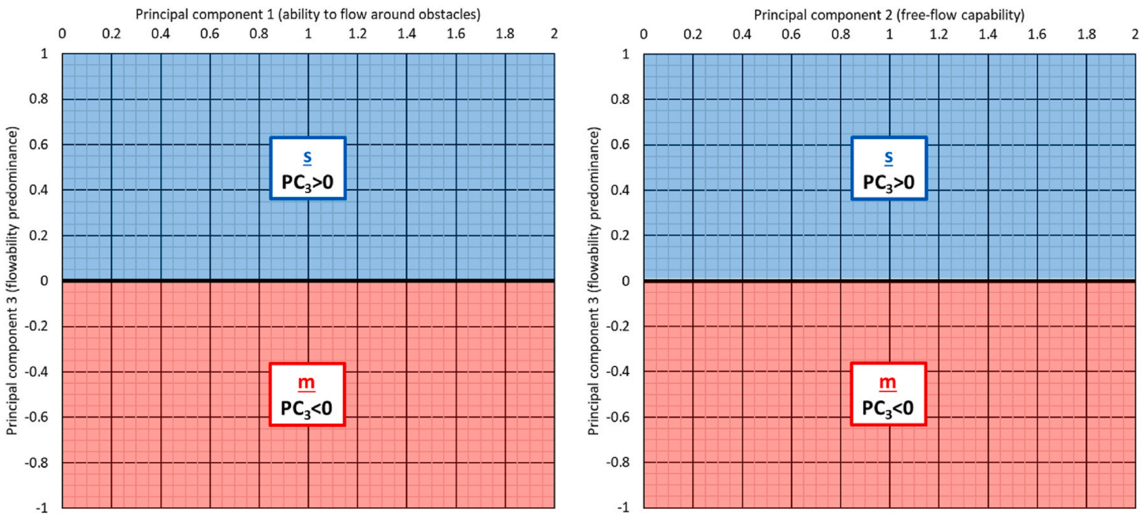

Fig. 7. Flowability-predominance zones.

- On the contrary, if the third principal component is less than 0, then the SCC with sustainable raw materials will be dominated by uniformity of flow, because the normalized values of the slump flow and L-box blocking ratio will be higher than the normalized values of the fresh properties related to viscosity. Such mixtures can be coded with an *"m"* (movement, uniformity of flow-predominance zone).

In the three-parameter flowability classification, the designation given for the two-parameter flowability classification is supplemented by adding an *"s"* ($PC_3 > 0$) or an *"m"* ($PC_3 < 0$) at the end (for example, 2Am or 3Bs). This additional term in the designation is related to the placement of SCC, because a *Class-s* SCC containing sustainable raw materials, in which rate of flow predominates, ensures that concreting is performed quickly, thus saving time and, indirectly, money [36]. On the other hand, a *Class-m* SCC containing sustainable raw materials guarantees successful pouring, although it may result in higher concreting costs, due to a lengthier filling time in comparison with the *Class*-s SCC [37].

3.6. Overview

In summary, determining the flowability classification for an SCC mixture containing sustainable materials can be obtained in a simple manner as follows:

1. Experimentally measure the values of slump flow, slump-flow viscosity (t_{500}), the V-funnel emptying time, and the L-box blocking ratio of the SCC mix.
2. Obtain the normalized fresh properties: normalized slump flow (Equation (1)), normalized slump-flow viscosity (Equation (2)), normalized V-funnel emptying time (Equation (3)), and normalized L-box blocking ratio (Equation (4)).

3. Calculate the first and the second principal components using Equation (5) and Equation (6), respectively.
4. Calculate the $|a|$ parameter value (Equation (8)).
5. Assign one overall-flowability zone (codes *1*, *2*, *3*, *4*, and *5*; Table 3 and Fig. 3) to the SCC mix depending on the $|a|$ parameter value.
6. Calculate the $|\alpha|$ parameter value (Equation (9)).
7. Assign the SCC mix a flowability-balance zone (codes *A*, *B*, *C*, *D*, and *E*; Table 4 and Fig. 4) as a function of the $|\alpha|$ parameter value.

   With these seven steps, the two-parameter flowability classification will be defined (Fig. 5).

8. Calculate the third principal component (PC_3, Equation (7)).
9. Assign the SCC mix a flowability-predominance zone (codes *s* and *m*; Fig. 7), based on the value of the third principal component.

   With these two last steps, the three-parameter flowability classification will have been defined for any SCC mix (Figs. 5 and 7).

4. Application and usefulness of the flowability classification

Having presented the proposed SCC flowability classification in the previous section, in this section its utility for proper description of the flowability of SCC containing sustainable raw materials is discussed.

4.1. Accurate flowability description of the SCC containing sustainable raw materials

As indicated in the introduction, the flowability patterns of SCC when sustainable aggregates or binders are added are unlike those of SCC made with conventional raw materials. It implies that, when adding any type of waste or industrial by-product, one fresh property may improve while another worsens [8]. Thus, with the existing classifications, in which each fresh property is individually addressed, it is difficult to know in some cases whether the flowability of the SCC improves or worsens with the addition of a sustainable raw material [14].

The proposed classification entails simultaneous consideration of all the fresh properties, which in turn enables precise descriptions of in-fresh behavior and flowability improvements noted when adding sustainable raw materials to SCC. The authors consider this aspect of great importance, due to the highly variable flowability behavior of SCC depending on the sustainable raw materials it contains. This variability is found in the presence of sustainable aggregates and binders and is even noted between SCC mixes containing the same sustainable aggregate or binder, as shown in Fig. 8 for sustainable coarse and fine aggregates and Fig. 9 for sustainable binders (for clarity, not all the articles shown in Table 2 for each sustainable raw material were considered in the development of these figures).

4.2. Analysis of the effect of different factors on the flowability of SCC

The proposed classification and description of SCC flowability levels can be used for the analysis of other factors and their effects on flowability through a global approach, without having to consider each property separately. Some of these factors are the addition of different wastes or by-products (sustainable raw materials), the modification of the initial conditions of the raw materials and the passage of time. All these aspects are addressed in this section through different examples related to two of the sustainable raw materials for which studies in the literature are more abundant (Table 2): recycled concrete aggregate and ground granulated blast furnace slag.

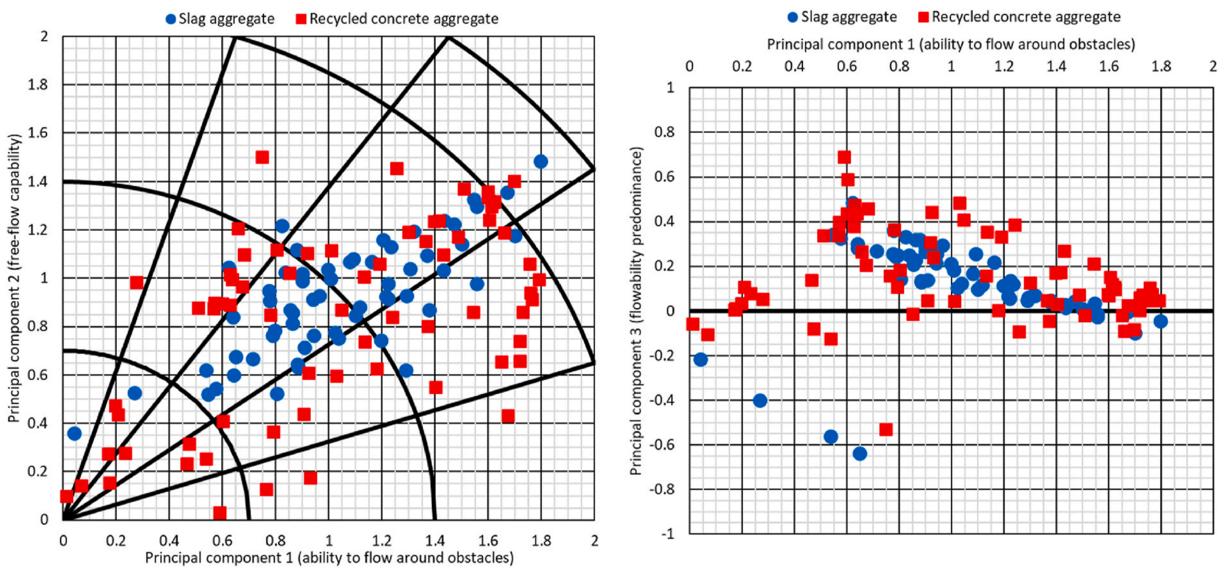

Fig. 8. Variability of flowability performance of SCC containing sustainable aggregates (see references list in Table 2).

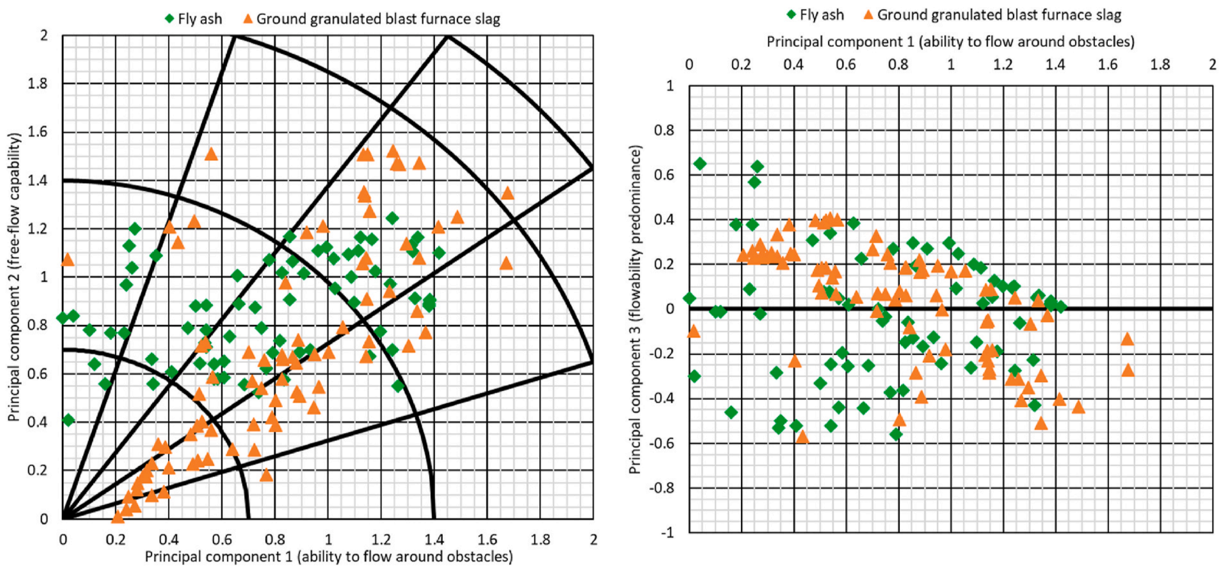

Fig. 9. Variability of flowability performance of SCC containing sustainable binders (see references list in Table 2).

4.2.1. Variation of the SCC composition

Fig. 10 shows the SCC flowability trends with increasing contents of recycled concrete aggregate in both the coarse and the fine fractions:

- On the one hand, it can be seen that the increase in the content of coarse recycled concrete aggregate mainly reduces the overall flowability of the SCC. Thus, in the example shown [25], the SCC was *Class 4 overall-flowability* for 0% coarse recycled concrete aggregate and *Class 5* when 50% was added. The irregular shape of this residue compared to natural aggregate [56] appeared to be the cause of a proportional reduction in all fresh properties, as there was no change in the flowability-balance class, so that the SCC was in all cases *Class B* (recommended use in gutter pouring and when concreting large elements with conventional reinforcement).
- On the other hand, increasing the content of fine recycled concrete aggregate tends to affect the rheology of the cement paste [8]. Thus, in the example given [37], raising this sustainable aggregate from 0% to 100% not only caused the overall-flowability class to vary from *3* to *4*, but also led to a notable increase of the imbalance in the flowability of the SCC. Thus, the SCC had a *Class A flowability-balance* (ideal) for 0% fine recycled concrete aggregate and a *Class D flowability-balance* for 100% fine recycled concrete aggregate. The SCC passed from an optimal balance between free-flow capability and ability to flow around obstacles with 0% fine recycled concrete aggregate to a much lower ability to flow around obstacles than its free-flow capability when adding 100% fine

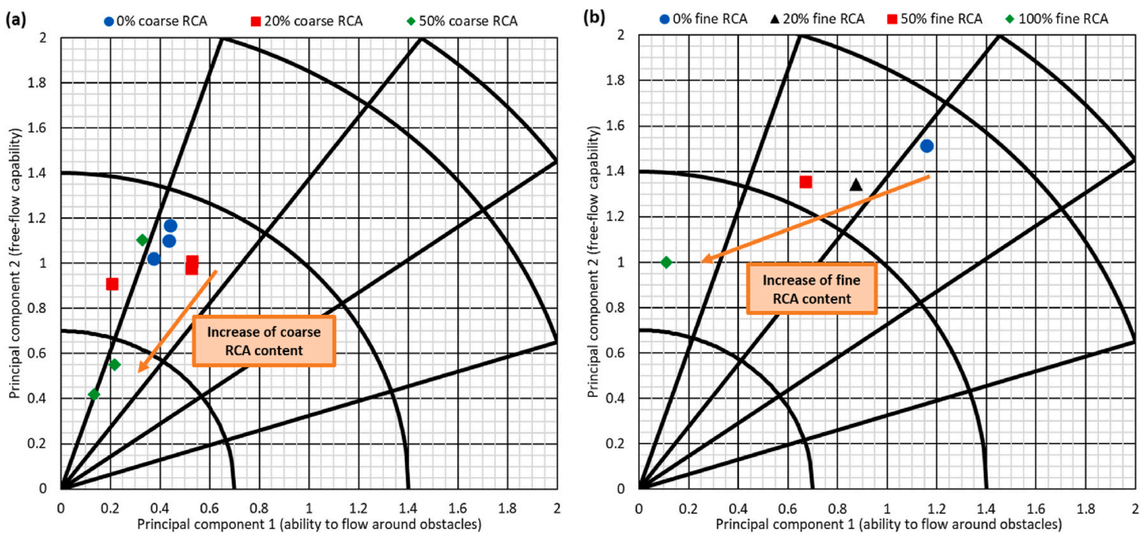

Fig. 10. Flowability evolution when varying the content of recycled concrete aggregate (RCA): (a) coarse fraction [25]; (b) fine fraction [37].

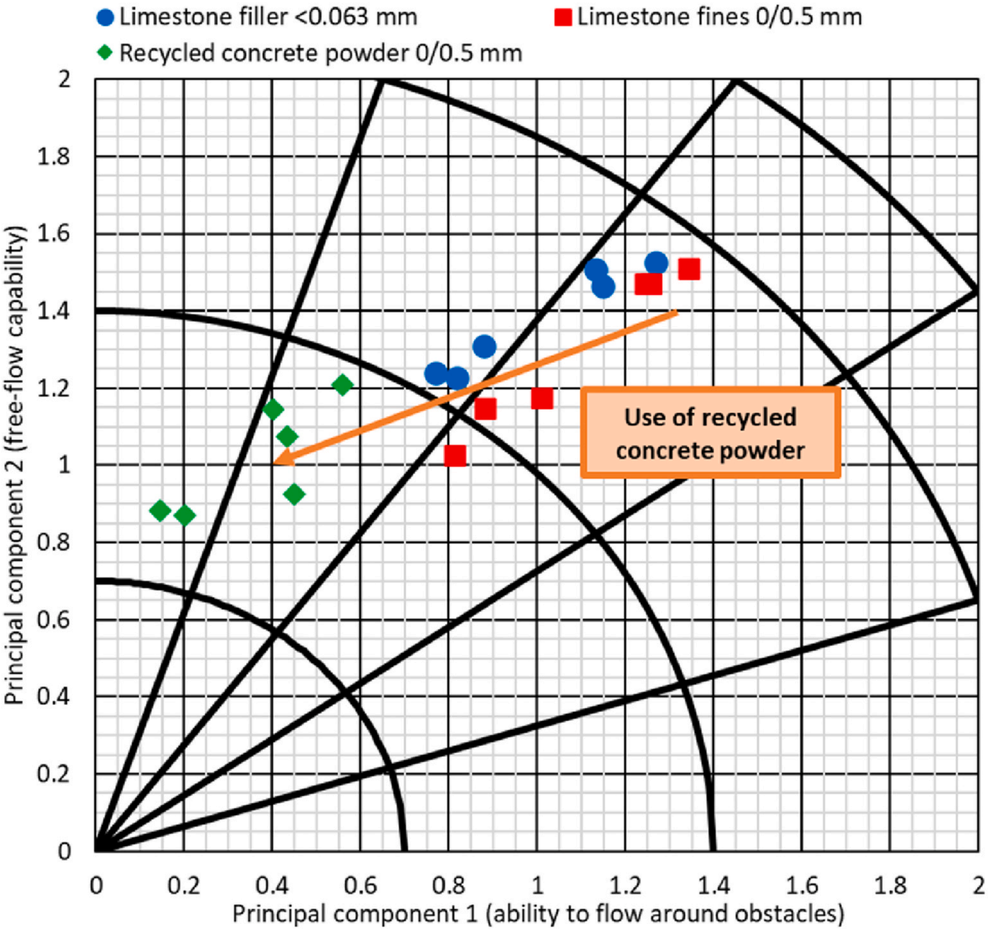

Fig. 11. Flowability evolution when modifying the nature of the aggregate powder [26].

recycled concrete aggregate. The behavior was exactly the same when limestone aggregate powders (aggregate fraction 0/0.5 mm added to SCC to reach self-compactability) were replaced with recycled concrete powder, as shown in Fig. 11 [26].

The same analysis can be performed when sustainable binders are used. In general, it is assumed that the use of this type of binders implies a worsening of the SCC flowability [32]. However, if the mix composition is adapted to the characteristics of each sustainable binder, this behavior can be different. Fig. 12 shows that ground granulated blast furnace slag can be successfully used, if the coarse aggregate content is reduced when this binder is added, due to its high grinding fineness compared to ordinary Portland cement [26]. In this way, it is possible to preserve the flowability-balance zone of SCC, and even improve its overall flowability.

4.2.2. Modification of the initial conditions of sustainable raw materials

Another factor whose influence on flowability can be analyzed is the initial state of the sustainable raw materials added to the SCC. Fig. 13 shows the effect of modifying the initial moisture of the coarse recycled concrete aggregate [25]. It can be observed that its modification mostly implies an alteration of the overall flowability of the SCC, as approximately all the SCC mixes, regardless of the initial moisture content of this sustainable aggregate, are found in the same flowability-balance zone. In addition, the difference between using the aggregate under oven-dried or environmental conditions never resulted in large ranges of SCC flowability, as the content of coarse recycled concrete aggregate increased. However, additions of coarse recycled concrete aggregate after pre-soaking resulted in better preservation of overall flowability as the amount of this sustainable aggregate increased.

4.2.3. Passage of time

Finally, Fig. 14 shows the usefulness of the proposed classification to analyze the effect of the passage of time, according to some results reported in the literature [37]. The workability of concrete decreases over time due to water evaporation and the setting process [11]. Thus, on the one hand, the passage of 30 min since the mixing end caused a decrease in overall flowability, so that the mixes went from an *overall-flowability Class 3* to an *overall-flowability Class 4*. It was nevertheless also observed that this decrease in flowability was not balanced, as there was a more pronounced decrease in the fresh properties linked to the ability to flow around obstacles (V-funnel emptying time and L-box blocking ratio). The mixes therefore changed their flowability-balance zone, moving from Class *B* to *Class D*.

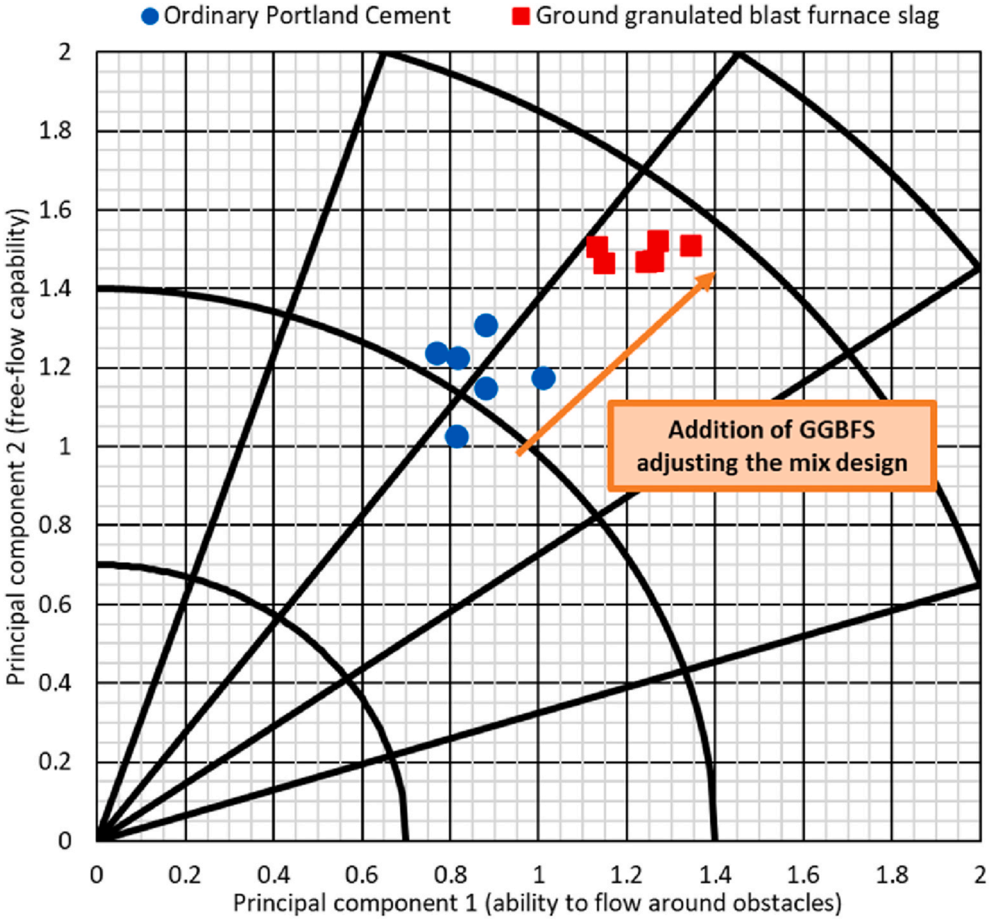

Fig. 12. Flowability evolution with additions of ground granulated blast furnace slag (GGBFS) adjusting the mix composition [26].

SCC with fine recycled concrete aggregate therefore lost a lot more of its ability to flow around obstacles than its free-flow capability.

5. Conclusions

In this paper a multi-parametric flowability classification for Self-Compacting Concrete (SCC) with sustainable raw materials has been developed by taking all the following fresh properties (slump flow, slump-flow viscosity, V-funnel emptying time, and L-box blocking ratio) simultaneously into consideration. The two main contributions of the flowability classification addressed in this paper are set out below:

- First, the flowability of any SCC mix with sustainable raw materials can be accurately described by considering overall-flowability zones, which quantify SCC flowability in absolute terms (Table 3 and Fig. 3), and flowability-balance zones, which evaluate the balance between the free-flow capability and the ability to flow around obstacles of the SCC mix (Table 4 and Fig. 4). Their simultaneous consideration is sufficient to reach the two-parameter flowability classification of the SCC mix (Fig. 5). However, for a more detailed flowability description, flowability-predominance zones, which indicate whether the rate or uniformity of flow predominates in the SCC mix, can also be considered (three-parameter flowability classification, Fig. 7).
- Second, the real applicability of any SCC mix with sustainable raw materials can be defined in the light of the suggested classification system. That applicability will depend on the overall-flowability and flowability-balance zones in which the mix is found. The overall flowability defines whether the SCC will exhibit adequate self-compactability during placement and therefore no vibration. The flowability balance determines whether the SCC will be suitable either for gutter pouring to produce conventional reinforced concrete components or for pumping to produce heavily reinforced concrete components.

From the development of the proposed multi-parametric classification, another three key points on the flowability of SCC with sustainable raw materials can be mentioned:

- The effect that each sustainable raw material on the flowability of the SCC may exhibit a high variability (Figs. 8 and 9). Therefore, the flowability of SCC containing sustainable raw materials cannot be clearly described by separately considering its fresh

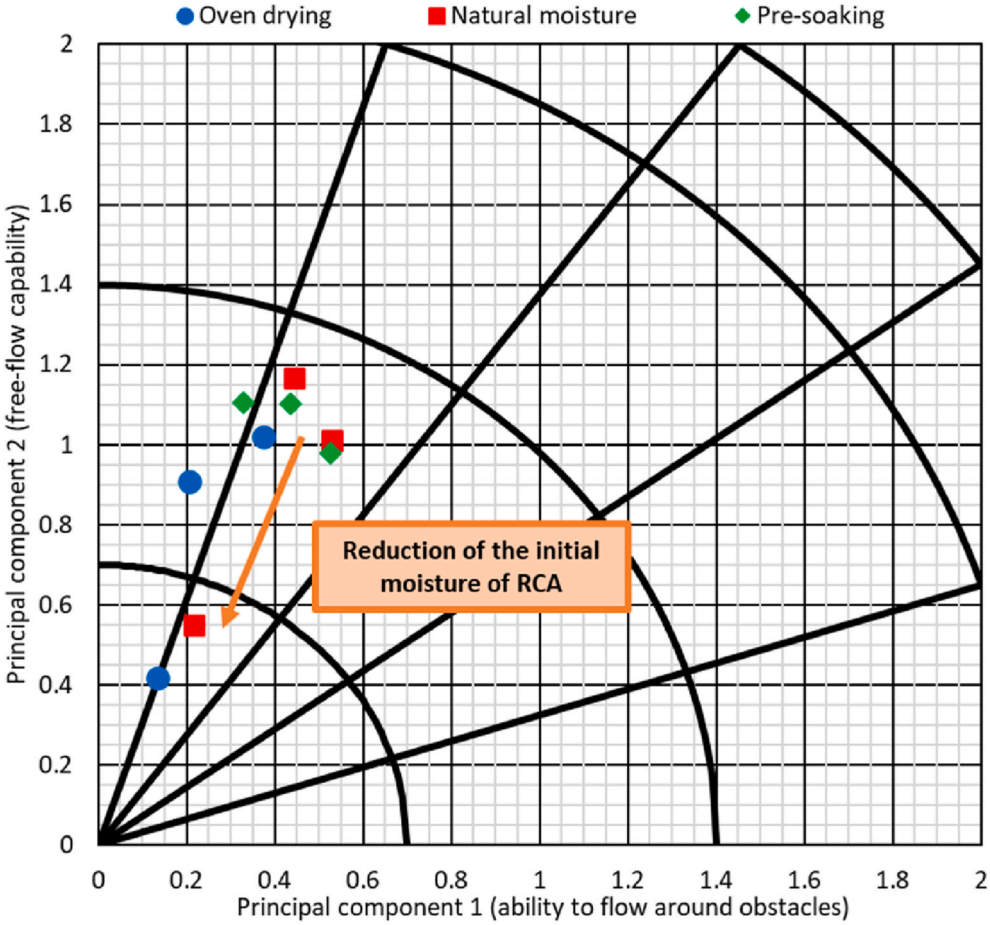

Fig. 13. Flowability evolution when modifying the initial moisture of coarse recycled concrete aggregate (RCA) [25].

properties. Interrelating all the fresh properties with each other is suggested for reaching a more complete and accurate description of SCC in-fresh behavior and its applicability.

- From the overall-flowability and flowability-balance zones, it can be stated that obtaining an SCC made from sustainable raw materials with optimal fresh behavior is not only conditional upon all fresh properties that are as high as possible. It also requires the existence of a balance between its free-flow capability (slump flow and slump-flow viscosity) and its ability to flow around obstacles (V-funnel emptying time and L-box blocking ratio). Thus, the mix design should be oriented towards the simultaneous achievement of both aspects.
- From the flowability-predominance zones, it is found that an SCC with better viscosity values compared to flow-related results (slump flow and L-box blocking ratio) will require less placement time, which will in turn reduce costs. However, the opposite situation ensures optimal formwork filling, although concreting may require extra time.

The authors consider that the proposed classification provides a clear and concise overview of the flowability of SCC containing sustainable raw materials. However, from an analysis of the studies within the knowledge base for the preparation of this classification (Table 2), it can be seen that SCC containing sustainable aggregates, such as slag aggregate and recycled concrete aggregate, and binders, such as fly ash, ground granulated blast furnace slag, and silica fume, predominate. The proposed classification is mainly adapted to those five sustainable raw materials. Studies are therefore advisable on the fresh behavior of SCC made with other less-intensively-studied sustainable raw materials, such as plastic aggregate, glass aggregate, different types of sustainable aggregate powder, and metakaolin. In this way, the greater availability of data may be used to complement the proposed classification widening both its validity and its fields of application.

CRediT authorship contribution statement

Víctor Revilla-Cuesta: Conceptualization, Investigation, Methodology, Data curation, Formal analysis, Software, Writing – original draft, Writing – review & editing. **Marta Skaf:** Conceptualization, Investigation, Formal analysis, Project administration, Resources, Writing – review & editing, Supervision. **Vanesa Ortega-López:** Conceptualization, Methodology, Project administration, Funding acquisition, Resources, Writing – review & editing, Supervision. **Juan M. Manso:** Conceptualization, Methodology, Project

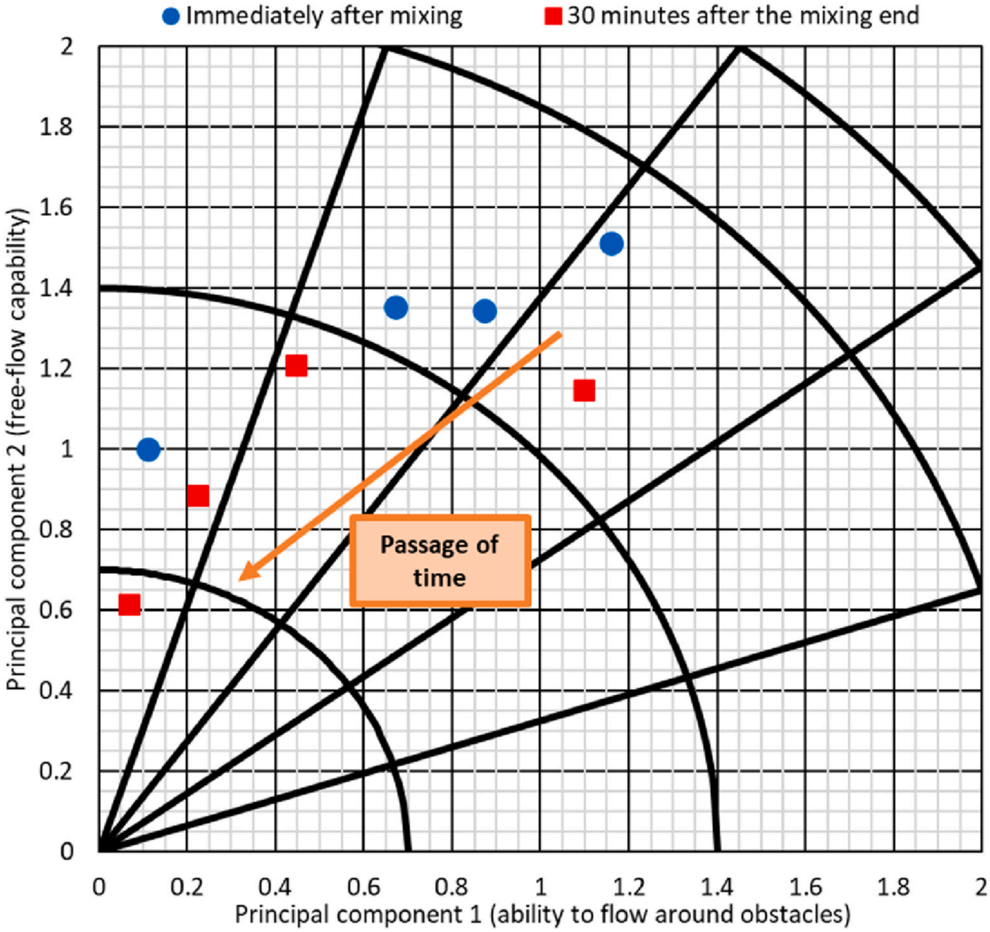

Fig. 14. Flowability trends of SCC containing fine recycled concrete aggregate [37].

administration, Funding acquisition, Resources, Writing – review & editing, Supervision.

Declaration of competing interest

The authors declare that they have no known competing financial interests or personal relationships that could have appeared to influence the work reported in this paper.

Data availability

Data will be made available on request.

Acknowledgements

This research work was supported by the Spanish Ministry of Universities, MICINN, AEI, EU, ERDF and NextGenerationEU/PRTR [grant numbers PID2020-113837RB-I00; 10.13039/501100011033; TED2021-129715B–I00; FPU17/03374]; the Junta de Castilla y León (Regional Government) and ERDF [grant number UIC-231]; and, finally, the University of Burgos [grant number SUCONS, Y135. GI].

References

[1] EFNARC, Specification Guidelines for Self-Compacting Concrete, European Federation of National Associations Representing producers and applicators of specialist building products for Concrete, 2002.

[2] V. Revilla-Cuesta, V. Ortega-López, M. Skaf, J.M. Manso, Effect of fine recycled concrete aggregate on the mechanical behavior of self-compacting concrete, Construct. Build. Mater. 263 (2020), 120671, https://doi.org/10.1016/j.conbuildmat.2020.120671.

[3] A.S. Reddy, P.R. Kumar, P.A. Raj, Development of sustainable performance index (SPI) for self-compacting concretes, J. Build. Eng. 27 (2020), 100974, https://doi.org/10.1016/j.jobe.2019.100974.

[4] B.R. Rajeshwari, M.V.N. Sivakumar, P.H. Praneeth, Visualization and quantification of aggregate and fiber in self-compacting concrete using computed tomography for wedge splitting test, Arch. Civ. Mech. Eng. 20 (4) (2020) 139, https://doi.org/10.1007/s43452-020-00140-z.
[5] M. Omrane, M. Rabehi, Effect of natural pozzolan and recycled concrete aggregates on thermal and physico-mechanical characteristics of self-compacting concrete, Construct. Build. Mater. 247 (2020), 118576, https://doi.org/10.1016/j.conbuildmat.2020.118576.
[6] En-Euronorm, Rue de stassart, 36. Belgium-1050 Brussels, European Committee for Standardization.
[7] V. Revilla-Cuesta, M. Skaf, F. Faleschini, J.M. Manso, V. Ortega-López, Self-compacting concrete manufactured with recycled concrete aggregate: an overview, J. Clean. Prod. 262 (2020), 121362, https://doi.org/10.1016/j.jclepro.2020.121362.
[8] S. Santos, P.R. da Silva, J. de Brito, Self-compacting concrete with recycled aggregates – a literature review, J. Build. Eng. 22 (2019) 349–371, https://doi.org/10.1016/j.jobe.2019.01.001.
[9] O. Sevim, İ. Kalkan, İ. Demir, A.P. Akgüngör, Effects of the sole or combined use of chemical admixtures on properties of self-compacting concrete, Arch. Civ. Mech. Eng. 21 (4) (2021) 150, https://doi.org/10.1007/s43452-021-00302-7.
[10] A. Santamaría, A. Orbe, M.M. Losañez, M. Skaf, V. Ortega-Lopez, J.J. González, Self-compacting concrete incorporating electric arc-furnace steelmaking slag as aggregate, Mater. Des. 115 (2017) 179–193, https://doi.org/10.1016/j.matdes.2016.11.048.
[11] H. Okamura, M. Ouchi, Self-compacting concrete, J. Adv. Concr. Technol. 1 (1) (2003) 5–15.
[12] A. Santamaría, J.J. González, M.M. Losáñez, M. Skaf, V. Ortega-López, The design of self-compacting structural mortar containing steelmaking slags as aggregate, Cem. Concr. Compos. 111 (2020), 103627, https://doi.org/10.1016/j.cemconcomp.2020.103627.
[13] K.H. Yang, Y.B. Jung, M.S. Cho, S.H. Tae, Effect of supplementary cementitious materials on reduction of CO2 emissions from concrete, J. Clean. Prod. 103 (2015) 774–783, https://doi.org/10.1016/j.jclepro.2014.03.018.
[14] N. Gupta, R. Siddique, R. Belarbi, Sustainable and greener self-compacting concrete incorporating industrial by-products: a review, J. Clean. Prod. 284 (2021), 124803, https://doi.org/10.1016/j.jclepro.2020.124803.
[15] M.U. Hossain, D. Xuan, S.T. Ng, B. Amor, Designing sustainable partition wall blocks using secondary materials: a life cycle assessment approach, J. Build. Eng. 43 (2021), 103035, https://doi.org/10.1016/j.jobe.2021.103035.
[16] R. Lanti, M. Martínez, Biaxial bending and axial load in reinforced concrete sections, Numerical aproach, Inf. Constr. 72 (558) (2020) 1–9, https://doi.org/10.3989/ic.69148.
[17] R. Sharma, R.A. Khan, Sustainable use of copper slag in self compacting concrete containing supplementary cementitious materials, J. Clean. Prod. 151 (2017) 179–192, https://doi.org/10.1016/j.jclepro.2017.03.031.
[18] Y. Sharifi, I. Afshoon, S. Asad-Abadi, F. Aslani, Environmental protection by using waste copper slag as a coarse aggregate in self-compacting concrete, J. Environ. Manag. 271 (2020), 111013, https://doi.org/10.1016/j.jenvman.2020.111013.
[19] A.S. Brand, E.O. Fanijo, A review of the influence of steel furnace slag type on the properties of cementitious composites, Appl. Sci. 10 (22) (2020) 8210, https://doi.org/10.3390/app10228210.
[20] A. Piemonti, A. Conforti, L. Cominoli, S. Sorlini, A. Luciano, G. Plizzari, Use of iron and steel slags in concrete: state of the art and future perspectives, Sustainability 13 (2) (2021) 556, https://doi.org/10.3390/su13020556.
[21] R.H. Faraj, H.F. Hama Ali, A.F.H. Sherwani, B.R. Hassan, H. Karim, Use of recycled plastic in self-compacting concrete: a comprehensive review on fresh and mechanical properties, J. Build. Eng. 30 (2020), 101283, https://doi.org/10.1016/j.jobe.2020.101283.
[22] N. Singh, P. Kumar, P. Goyal, Reviewing the behaviour of high volume fly ash based self compacting concrete, J. Build. Eng. 26 (2019), 100882, https://doi.org/10.1016/j.jobe.2019.100882.
[23] K. Devi, P. Aggarwal, B. Saini, Admixtures used in self-compacting concrete: a review, Iran, J. Sci. Tech. Trans. Civ. Eng. 44 (2) (2020) 377–403, https://doi.org/10.1007/s40996-019-00244-4.
[24] D. Dominguez-Santos, Structural performance of concrete blocks with wood aggregates for the construction of medium and high-rise buildings, Inf. Constr. 73 (564) (2021) e414, https://doi.org/10.3989/IC.81319.
[25] I. González-Taboada, B. González-Fonteboa, J. Eiras-López, G. Rojo-López, Tools for the study of self-compacting recycled concrete fresh behaviour: workability and rheology, J. Clean. Prod. 156 (2017) 1–18, https://doi.org/10.1016/j.jclepro.2017.04.045.
[26] V. Revilla-Cuesta, M. Skaf, A. Santamaría, J.J. Hernández-Bagaces, V. Ortega-López, Temporal flowability evolution of slag-based self-compacting concrete with recycled concrete aggregate, J. Clean. Prod. 299 (2021), 126890, https://doi.org/10.1016/j.jclepro.2021.126890.
[27] H. Qasrawi, Hardened properties of green self-consolidating concrete made with steel slag coarse aggregates under hot conditions, ACI Mater. J. 117 (1) (2020) 107–118, https://doi.org/10.14359/51719072.
[28] S. Rehman, S. Iqbal, A. Ali, Combined influence of glass powder and granular steel slag on fresh and mechanical properties of self-compacting concrete, Construct. Build. Mater. 178 (2018) 153–160, https://doi.org/10.1016/j.conbuildmat.2018.05.148.
[29] L.R.R. da Silva, J.A. da Silva, M.B. Francisco, V.A. Ribeiro, M.H.B. de Souza, P. Capellato, M.A. Souza, V.C. Dos Santos, P.C. Gonçalves, M.L.N.M. Melo, Polymeric waste from recycling refrigerators as an aggregate for self-compacting concrete, Sustainability 12 (20) (2020) 8731, https://doi.org/10.3390/su12208731.
[30] R.H. Faraj, A.F.H. Sherwani, L.H. Jafer, D.F. Ibrahim, Rheological behavior and fresh properties of self-compacting high strength concrete containing recycled PP particles with fly ash and silica fume blended, J. Build. Eng. 34 (2021), 101667, https://doi.org/10.1016/j.jobe.2020.101667.
[31] Y. Ouldkhaoua, B. Benabed, R. Abousnina, E.H. Kadri, J. Khatib, Effect of using metakaolin as supplementary cementitious material and recycled CRT funnel glass as fine aggregate on the durability of green self-compacting concrete, Construct. Build. Mater. 235 (2020), 117802, https://doi.org/10.1016/j.conbuildmat.2019.117802.
[32] A. Beycioǻlu, H. Yilmaz Aruntaş, Workability and mechanical properties of self-compacting concretes containing LLFA, GBFS and MC, Construct. Build. Mater. 73 (2014) 626–635, https://doi.org/10.1016/j.conbuildmat.2014.09.071.
[33] M. Behera, A.K. Minocha, S.K. Bhattacharyya, Flow behavior, microstructure, strength and shrinkage properties of self-compacting concrete incorporating recycled fine aggregate, Construct. Build. Mater. 228 (2019), 116819, https://doi.org/10.1016/j.conbuildmat.2019.116819.
[34] R. Manjunath, M.C. Narasimhan, K.M. Umesh, K. Shivam, U.K. Bala Bharathi, Studies on development of high performance, self-compacting alkali activated slag concrete mixes using industrial wastes, Construct. Build. Mater. 198 (2019) 133–147, https://doi.org/10.1016/j.conbuildmat.2018.11.242.
[35] D. Karthik, K. Nirmalkumar, R. Priyadharshini, Characteristic assessment of self-compacting concrete with supplementary cementitious materials, Construct. Build. Mater. 297 (2021), 123845, https://doi.org/10.1016/j.conbuildmat.2021.123845.
[36] I. González-Taboada, B. González-Fonteboa, F. Martínez-Abella, D. Carro-López, Self-compacting recycled concrete: relationships between empirical and rheological parameters and proposal of a workability box, Construct. Build. Mater. 143 (2017) 537–546, https://doi.org/10.1016/j.conbuildmat.2017.03.156.
[37] D. Carro-López, B. González-Fonteboa, J. De Brito, F. Martínez-Abella, I. González-Taboada, P. Silva, Study of the rheology of self-compacting concrete with fine recycled concrete aggregates, Construct. Build. Mater. 96 (2015) 491–501, https://doi.org/10.1016/j.conbuildmat.2015.08.091.
[38] R. Sharma, R.A. Khan, Durability assessment of self compacting concrete incorporating copper slag as fine aggregates, Construct. Build. Mater. 155 (2017) 617–629, https://doi.org/10.1016/j.conbuildmat.2017.08.074.
[39] N. Gupta, R. Siddique, Strength and micro-structural properties of self-compacting concrete incorporating copper slag, Construct. Build. Mater. 224 (2019) 894–908, https://doi.org/10.1016/j.conbuildmat.2019.07.105.
[40] P. Chandru, J. Karthikeyan, A.K. Sahu, K. Sharma, C. Natarajan, Performance evaluation between ternary blended SCC mixes containing induction furnace slag and crushed stone as coarse aggregate, Construct. Build. Mater. 267 (2021), 120953, https://doi.org/10.1016/j.conbuildmat.2020.120953.
[41] R. Sharma, R.A. Khan, Sulfate resistance of self compacting concrete incorporating copper slag as fine aggregates with mineral admixtures, Construct. Build. Mater. 287 (2021), 122985, https://doi.org/10.1016/j.conbuildmat.2021.122985.
[42] P. Abhishek, P. Ramachandra, P.S. Niranjan, Use of recycled concrete aggregate and granulated blast furnace slag in self-compacting concrete, Mater. Today Proc. 42 (2020) 479–486, https://doi.org/10.1016/j.matpr.2020.10.239.

[43] B. Krishna Chaitanya, I. Sivakumar, Influence of waste copper slag on flexural strength properties of self compacting concrete, Mater. Today Proc. 42 (2020) 671–676, https://doi.org/10.1016/j.matpr.2020.11.059.
[44] A. Sambangi, E. Arunakanthi, Fresh and mechanical properties of SCC with fly ash and copper slag as mineral admixtures, Mater. Today Proc. 45 (2020) 6687–6693, https://doi.org/10.1016/j.matpr.2020.12.144.
[45] R. Manjunath, M.C. Narasimhan, An experimental investigation on self-compacting alkali activated slag concrete mixes, J. Build. Eng. 17 (2018) 1–12, https://doi.org/10.1016/j.jobe.2018.01.009.
[46] M. Nuruzzaman, J.O. Camargo Casimiro, P.K. Sarker, Fresh and hardened properties of high strength self-compacting concrete using by-product ferronickel slag fine aggregate, J. Build. Eng. 32 (2020), 101686, https://doi.org/10.1016/j.jobe.2020.101686.
[47] I. Sosa, C. Thomas, J.A. Polanco, J. Setién, P. Tamayo, High performance self-compacting concrete with electric arc furnace slag aggregate and cupola slag powder, Appl. Sci. 10 (3) (2020) 773, https://doi.org/10.3390/app10030773.
[48] P. Murthi, K. Poongodi, P.O. Awoyera, R. Gobinath, K.T. Raja, O.B. Olalusi, Fresh properties of self-compacting concrete incorporating electric arc furnace oxidizing slag (EAFOS) as coarse aggregate, SN Appl. Sci. 2 (4) (2020) 651, https://doi.org/10.1007/s42452-020-2497-6.
[49] T. Ali-Boucetta, M. Behim, F. Cassagnabere, M. Mouret, A. Ayat, W. Laifa, Durability of self-compacting concrete containing waste bottle glass and granulated slag, Construct. Build. Mater. 270 (2021), 121133, https://doi.org/10.1016/j.conbuildmat.2020.121133.
[50] C. Sun, Q. Chen, J. Xiao, W. Liu, Utilization of waste concrete recycling materials in self-compacting concrete, Resour. Conserv. Recycl. 161 (2020), 104930, https://doi.org/10.1016/j.resconrec.2020.104930.
[51] Z. Duan, A. Singh, J. Xiao, S. Hou, Combined use of recycled powder and recycled coarse aggregate derived from construction and demolition waste in self-compacting concrete, Construct. Build. Mater. 254 (2020), 119323, https://doi.org/10.1016/j.conbuildmat.2020.119323.
[52] B.S. Saini, S.P. Singh, Flexural fatigue strength prediction of self compacting concrete made with recycled concrete aggregates and blended cements, Construct. Build. Mater. 264 (2020), 120233, https://doi.org/10.1016/j.conbuildmat.2020.120233.
[53] R.B. Singh, S. Debbarma, N. Kumar, S. Singh, Hardened state behaviour of self-compacting concrete pavement mixes containing alternative aggregates and secondary binders, Construct. Build. Mater. 266 (2021), 120624, https://doi.org/10.1016/j.conbuildmat.2020.120624.
[54] K. Kapoor, S.P. Singh, B. Singh, P. Singh, Effect of recycled aggregates on fresh and hardened properties of self compacting concrete, Mater. Today Proc. 32 (2020) 600–607, https://doi.org/10.1016/j.matpr.2020.02.753.
[55] N. Bahrami, M. Zohrabi, S.A. Mahmoudy, M. Akbari, Optimum recycled concrete aggregate and micro-silica content in self-compacting concrete: rheological, mechanical and microstructural properties, J. Build. Eng. 31 (2020), 101361, https://doi.org/10.1016/j.jobe.2020.101361.
[56] F. Fiol, C. Thomas, C. Muñoz, V. Ortega-López, J.M. Manso, The influence of recycled aggregates from precast elements on the mechanical properties of structural self-compacting concrete, Construct. Build. Mater. 182 (2018) 309–323, https://doi.org/10.1016/j.conbuildmat.2018.06.132.
[57] S.A. Santos, P.R. da Silva, J. de Brito, Mechanical performance evaluation of self-compacting concrete with fine and coarse recycled aggregates from the precast industry, Materials 10 (8) (2017) 904, https://doi.org/10.3390/ma10080904.
[58] B.M. Vinay Kumar, H. Ananthan, K.V.A. Balaji, Experimental studies on utilization of coarse and finer fractions of recycled concrete aggregates in self compacting concrete mixes, J. Build. Eng. 9 (2017) 100–108, https://doi.org/10.1016/j.jobe.2016.11.013.
[59] T. Barroqueiro, P.R. da Silva, J. de Brito, High-performance self-compacting concrete with recycled aggregates from the precast industry: durability assessment, Buildings 10 (6) (2020) 113, https://doi.org/10.3390/BUILDINGS10060113.
[60] K. Kapoor, S.P. Singh, B. Singh, Evaluating the durability properties of self compacting concrete made with coarse and fine recycled concrete aggregates, Eur. J. Environ. Civ. Eng. 24 (14) (2020) 2383–2399, https://doi.org/10.1080/19648189.2018.1506825.
[61] K. Nandanam, U.S. Biswal, P. Dinakar, Effect of fly ash, GGBS, and metakaolin on mechanical and durability properties of self-compacting concrete made with 100% coarse recycled aggregate, J. Hazard. Toxic Radioact. Waste 25 (2) (2021), https://doi.org/10.1061/(ASCE)HZ.2153-5515.0000595, 04021002-1.
[62] K. Kapoor, S.P. Singh, B. Singh, Improving the durability properties of self-consolidating concrete made with recycled concrete aggregates using blended cements, Int. J. Civ. Eng. 19 (7) (2021) 759–775, https://doi.org/10.1007/s40999-020-00584-7.
[63] V. Revilla-Cuesta, M. Skaf, A.B. Espinosa, A. Santamaría, V. Ortega-López, Statistical approach for the design of structural self-compacting concrete with fine recycled concrete aggregate, Mathematics 8 (12) (2020) 2190, https://doi.org/10.3390/math8122190.
[64] K. Kapoor, S.P. Singh, B. Singh, Permeability of self-compacting concrete made with recycled concrete aggregates and Portland cement-fly ash-silica fume binder, J. Sustain. Cem. Based Mater. 10 (4) (2021) 213–239, https://doi.org/10.1080/21650373.2020.1809029.
[65] R.B. Ardalan, Z.N. Emamzadeh, H. Rasekh, A. Joshaghani, B. Samali, Physical and mechanical properties of polymer modified self-compacting concrete (SCC) using natural and recycled aggregates, J. Sustain. Cem. Based Mater. 9 (1) (2020) 1–16, https://doi.org/10.1080/21650373.2019.1666060.
[66] Z. Pan, J. Zhou, X. Jiang, Y. Xu, R. Jin, J. Ma, Y. Zhuang, Z. Diao, S. Zhang, Q. Si, W. Chen, Investigating the effects of steel slag powder on the properties of self-compacting concrete with recycled aggregates, Construct. Build. Mater. 200 (2019) 570–577, https://doi.org/10.1016/j.conbuildmat.2018.12.150.
[67] N. Hilal, N. Hamah Sor, R.H. Faraj, Development of eco-efficient lightweight self-compacting concrete with high volume of recycled EPS waste materials, Environ. Sci. Pollut. Res. 28 (2021) 50028–50051, https://doi.org/10.1007/s11356-021-14213-w.
[68] A. Hasan-Ghasemi, M. Nematzadeh, Tensile and compressive behavior of self-compacting concrete incorporating PET as fine aggregate substitution after thermal exposure: experiments and modeling, Construct. Build. Mater. 289 (2021), 123067, https://doi.org/10.1016/j.conbuildmat.2021.123067.
[69] A.H. Medher, A.I. Al-Hadithi, N. Hilal, The possibility of producing self-compacting lightweight concrete by using expanded polystyrene beads as coarse aggregate, Arabian J. Sci. Eng. 46 (5) (2021) 4253–4270, https://doi.org/10.1007/s13369-020-04886-9.
[70] L. Tian, L. Qiu, J. Li, Y. Yang, Experimental study of waste tire rubber, wood-plastic particles and shale ceramsite on the performance of self-compacting concrete, J. Renew. Mater. 8 (2) (2020) 153–170, https://doi.org/10.32604/jrm.2020.08701.
[71] B.R.K. Chunchu, J. Putta, Effect of recycled plastic granules as a partial substitute for natural resource sand on the durability of SCC, Resources 8 (3) (2019) 133, https://doi.org/10.3390/resources8030133.
[72] S. Rahat Dahmardeh, M.S. Sargazi Moghaddam, M.H. Mirabi Moghaddam, Effects of waste glass and rubber on the SCC: rheological, mechanical, and durability properties, Eur. J. Environ. Civ. Eng. 25 (2) (2021) 302–321, https://doi.org/10.1080/19648189.2018.1528891.
[73] A. Saha, M.H.R. Sobuz, M.I. Hoque, R. Mujahid, Influence of waste glass aggregates on the rheological properties of self-consolidated concrete, Aust. J. Civ. Eng. 18 (2) (2020) 272–285, https://doi.org/10.1080/14488353.2020.1785666.
[74] O.M.G. Al-Kerttani, Fresh and shrinkage properties of self-compacted concrete when using recycled glass as aggregate, Struct. Concr. 19 (4) (2018) 1245–1254, https://doi.org/10.1002/suco.201700069.
[75] J. Mallek, A. Daoud, O. Omikrine-Metalssi, A. Loulizi, Performance of self-compacting rubberized concrete against carbonation and chloride penetration, Struct. Concr. 22 (2021) 2720–2735, https://doi.org/10.1002/suco.202000687.
[76] A.F. Angelin, R.C. Cecche Lintz, W.R. Osório, L.A. Gachet, Evaluation of efficiency factor of a self-compacting lightweight concrete with rubber and expanded clay contents, Construct. Build. Mater. 257 (2020), 119573, https://doi.org/10.1016/j.conbuildmat.2020.119573.
[77] S.M. Mousavi Alizadeh, A. Rezaeian, I. Rasoolan, B. Tahmouresi, Compressive stress-strain model and residual strength of self-compacting concrete containing recycled ceramic aggregate after exposure to fire, J. Build. Eng. 38 (2021), 102206, https://doi.org/10.1016/j.jobe.2021.102206.
[78] S.T. Aly, A.S. El-Dieb, M.R. Taha, Effect of high-volume ceramic waste powder as partial cement replacement on fresh and compressive strength of self-compacting concrete, J. Mater. Civ. Eng. 31 (2) (2019), 04018374, https://doi.org/10.1061/(ASCE)MT.1943-5533.0002588.
[79] A. Singh, S. Arora, V. Sharma, B. Bhardwaj, Workability retention and strength development of self-compacting recycled aggregate concrete using ultrafine recycled powders and silica fume, J. Hazard. Toxic Radioact. Waste 23 (4) (2019), 04019016, https://doi.org/10.1061/(ASCE)HZ.2153-5515.0000456.
[80] V. Gokulnath, B. Ramesh, K. Priyadharsan, Study on m-sand in self compacting concrete with addition of glass powder in m-25 grade - a review, Mater, Today Proc 22 (2020) 659–662, https://doi.org/10.1016/j.matpr.2019.09.040.
[81] V. Gokulnath, B. Ramesh, S. Suvesha, Influence on flexural properties of glass powder in self compacting concrete, Mater, Today Proc 22 (2020) 788–792, https://doi.org/10.1016/j.matpr.2019.10.153.

[82] G.F. Huseien, A.R.M. Sam, K.W. Shah, J. Mirza, Effects of ceramic tile powder waste on properties of self-compacted alkali-activated concrete, Construct. Build. Mater. 236 (2020), 117574, https://doi.org/10.1016/j.conbuildmat.2019.117574.
[83] J. Mansoor, S.A.R. Shah, M.M. Khan, A.N. Sadiq, M.K. Anwar, M.U. Siddiq, H. Ahmad, Analysis of mechanical properties of self compacted concrete by partial replacement of cement with industrial wastes under elevated temperature, Appl. Sci. 8 (3) (2018) 364, https://doi.org/10.3390/app8030364.
[84] P. Hemalatha, K. Ramujee, Influence of nano material (TiO2) on self compacting Geo polymer concrete containing Flyash, GGBS and wollastonite, Mater. Today Proc. 43 (2020) 2438–2442, https://doi.org/10.1016/j.matpr.2021.02.279.
[85] N.V. K, D.L.V. Babu, Assessing the performance of molarity and alkaline activator ratio on engineering properties of self-compacting alkaline activated concrete at ambient temperature, J. Build. Eng. 20 (2018) 137–155, https://doi.org/10.1016/j.jobe.2018.07.005.
[86] Y.J. Patel, N. Shah, Development of self-compacting geopolymer concrete as a sustainable construction material, Sustainable Envir. Res. 28 (6) (2018) 412–421, https://doi.org/10.1016/j.serj.2018.08.004.
[87] M.A. Mirgozar Langaroudi, Y. Mohammadi, Effect of nano-clay on the freeze–thaw resistance of self-compacting concrete containing mineral admixtures, Eur. J. Environ. Civ. Eng. 26 (2) (2019) 481–500, https://doi.org/10.1080/19648189.2019.1665107.
[88] B.V. Kavyateja, J.G. Jawahar, C. Sashidhara, Durability performance of self compacting concrete incorporating alccofine and fly ash, Int. J. Eng. Trans. B Applic. 33 (8) (2020) 1522–1528, https://doi.org/10.5829/ije.2020.33.08b.10.
[89] V.K. Nagaraj, D.L. Venkatesh Babu, Formulation and performance evaluation of alkali-activated self-compacting concrete, Asian J. Civ. Eng. 19 (8) (2018) 1021–1036, https://doi.org/10.1007/s42107-018-0081-9.
[90] O.M. Ofuyatan, A.G. Adeniyi, D. Ijie, J.O. Ighalo, J. Oluwafemi, Development of high-performance self compacting concrete using eggshell powder and blast furnace slag as partial cement replacement, Construct. Build. Mater. 256 (2020), 119403, https://doi.org/10.1016/j.conbuildmat.2020.119403.
[91] A.A.A. Al-Oran, N.A. Safiee, N.A.M. Nasir, Fresh and hardened properties of self-compacting concrete using metakaolin and GGBS as cement replacement, Eur. J. Environ. Civ. Eng. 26 (1) (2019) 379–392, https://doi.org/10.1080/19648189.2019.1663268.
[92] I.A. Shabtai, L.M. Lynch, Y.G. Mishael, Designing clay-polymer nanocomposite sorbents for water treatment: a review and meta-analysis of the past decade, Water Res. 188 (2021), 116571, https://doi.org/10.1016/j.watres.2020.116571.
[93] S. Ebrahimzadeh, B. Wols, A. Azzellino, B.J. Martijn, J.P. van der Hoek, Quantification and modelling of organic micropollutant removal by reverse osmosis (RO) drinking water treatment, J. Water Proc. Eng. 42 (2021), 102164, https://doi.org/10.1016/j.jwpe.2021.102164.